

This is a repository copy of *Work-distribution quantumness and irreversibility when crossing a quantum phase transition in finite time*.

White Rose Research Online URL for this paper:

<https://eprints.whiterose.ac.uk/id/eprint/163028/>

Version: Accepted Version

Article:

Zawadzki, Krissia, Serra, Roberto M. and D'Amico, Irene orcid.org/0000-0002-4794-1348 (2020) Work-distribution quantumness and irreversibility when crossing a quantum phase transition in finite time. Physical Review Research. 033167. ISSN: 2643-1564

<https://doi.org/10.1103/PhysRevResearch.2.033167>

Reuse

Items deposited in White Rose Research Online are protected by copyright, with all rights reserved unless indicated otherwise. They may be downloaded and/or printed for private study, or other acts as permitted by national copyright laws. The publisher or other rights holders may allow further reproduction and re-use of the full text version. This is indicated by the licence information on the White Rose Research Online record for the item.

Takedown

If you consider content in White Rose Research Online to be in breach of UK law, please notify us by emailing eprints@whiterose.ac.uk including the URL of the record and the reason for the withdrawal request.

Supplemental Material – Work-distribution quantumness and irreversibility when crossing a quantum phase transition in finite time

Krissia Zawadzki,^{1,2} Roberto M. Serra,³ and Irene D’Amico^{4,1,5}

¹*Departamento de Física e Ciência Interdisciplinar,
Instituto de Física de São Carlos, University of São Paulo,
Caixa Postal 369, 13560-970 São Carlos, SP, Brazil*

²*Department of Physics, Northeastern University, Boston, Massachusetts 02115, USA*

³*Centro de Ciências Naturais e Humanas, Universidade Federal do ABC,
Avenida dos Estados 5001, 09210-580, Santo André, São Paulo, Brazil*

⁴*Department of Physics, University of York, York, YO10 5DD, United Kingdom*

⁵*International Institute of Physics, Federal University of Rio Grande do Norte, Natal, Brazil*

Evolution of work probability distribution

In our letter, we presented 3-dimensional plots for the evolution of the work probability distributions $P(W)$ with respect to the driving time τ , for chains of sizes $L = 4$ and $L = 8$ within zero and strong-coupling regimes, $U = 0J$ and $U = 10J$ respectively.

Here, we provide animations showing $P(W)$ evolving with τ , $\tau J = 0.2, \dots, 1.0, 1.5, 2.0, \dots, 10.0$, for fixed value of U ($U/J = 0.0, 1.0, 2.0, \dots, 10.0$) and for all the considered chain lengths, $2 \leq L \leq 8$. The animations clearly show how the distribution is strongly τ -dependent below the pM-QPT (weak many-body correlations), to become basically τ -independent above the pM-QPT (strong many-body correlations). These animations are available in the Figs named [work_distribution_beta=0.4_L=NSITES_U=COULOMB.gif](#), with NSITES=2,4,6,8 and COULOMB varying according to the range U/J above.

Moments of the quantum work probability distribution

As discussed in our letter, the statistics of the quantum work distribution $P(W)$ can be characterized by its momenta. Of particular importance are: its average $\langle W \rangle$; standard deviation $\langle W - \bar{W} \rangle^2$; and skewness, or third central momentum $\langle W - \bar{W} \rangle^3$. Here we present the heatmaps of these quantities – and in addition of the kurtosis, or fourth central momentum $\langle W - \bar{W} \rangle^4$ – with respect to U and τ , and for all considered system sizes $L = 2, 4, 6, 8$, see Figs. 1–4. To facilitate the comparison, we include here also the skewness for $L = 4$ and $L = 8$, already presented in the main text.

The heatmaps of the work produced by applying the external electric field is shown in panel (a) of Figs. 1–4, for $0 \leq U \leq 10J$ and $0.2/J \leq \tau \leq 10$. The freezing of the system due to the pM-QPT results in a dramatic reduction in the extractable work for all values of L .

For $L = 4, 6, 8$ the first four momenta of $P(W)$ display a *qualitative* behaviour which is size-independent, with the white lines in the heatmaps for the skewness $k = 3$ representing the points at which this quantity is zero. Also, for the same L , standard deviation and kurtosis have qualitatively similar behaviours.

However, for $L = 2$, the skewness remains negative for all coupling regimes U and driving times τ , while the kurtosis displays a behaviour qualitatively different from the standard deviation for weak interactions and intermediate to long driving times.

Entropy production

The entropy production corresponding to the average quantum work produced for $L = 4$ and $L = 8$ is plotted in Fig. 5, left and right panel, respectively. For low-correlations the entropy is strongly sensitive to the dynamical regime, and decreases as the system becomes more adiabatic. Note that, for a finite quantum system, adiabaticity does not imply equilibration, so the entropy is expected to remain finite for increasing τ . At high correlations, the entropy remains relatively low independently of τ .

The overall entropy behavior implies that, for the same type of driving potential and same driving time, tailoring many-body interactions may be used to approach – or not – equilibrium.

The entropy production not scaled by the system size ($\langle \Sigma \rangle / L$ is shown in the main text alongside with the trace distance between the final and the equilibrium state and the skewness of the distribution) as a function of U for

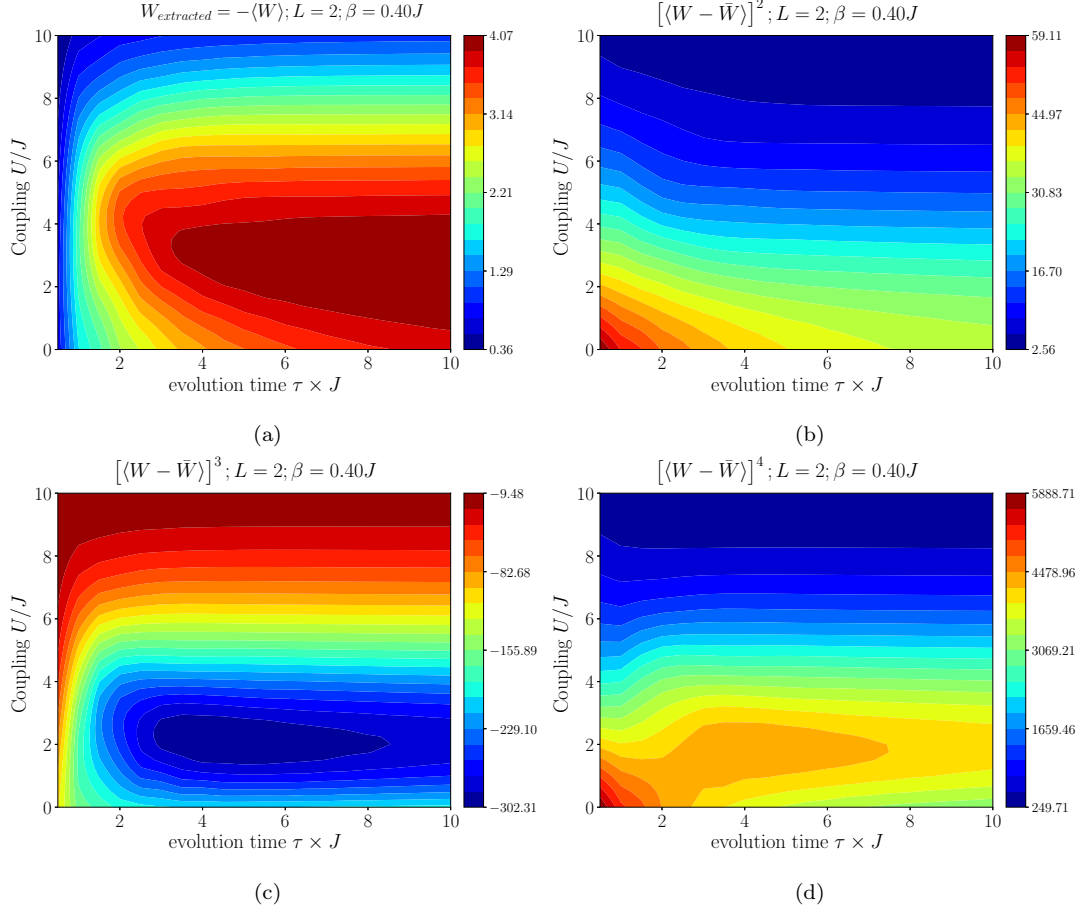


Figure 1: Heatmaps of the average work and the following three central momenta $\langle W - \bar{W} \rangle^k$ $k = 2, 3, 4$ for $L = 2$.

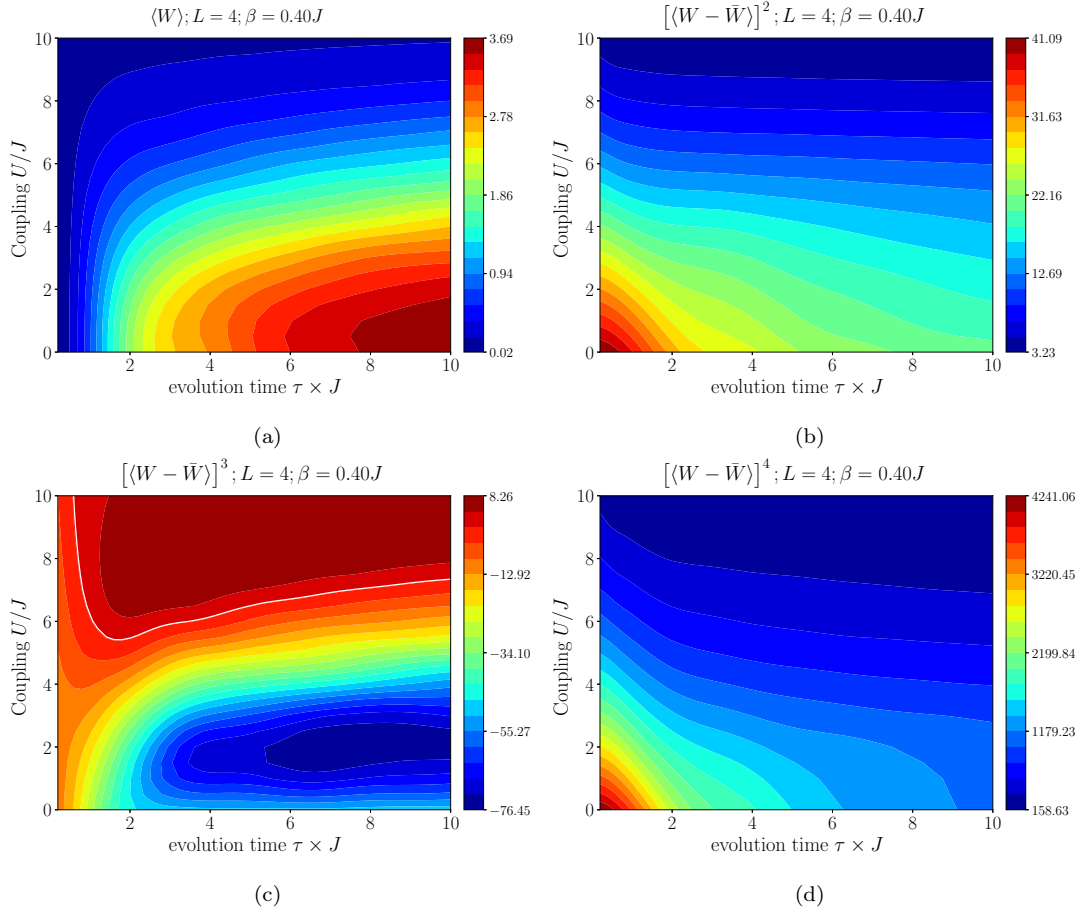


Figure 2: Heatmaps of the average work and the following three central momenta $\langle W - \bar{W} \rangle^k$ $k = 2, 3, 4$ for $L = 4$.

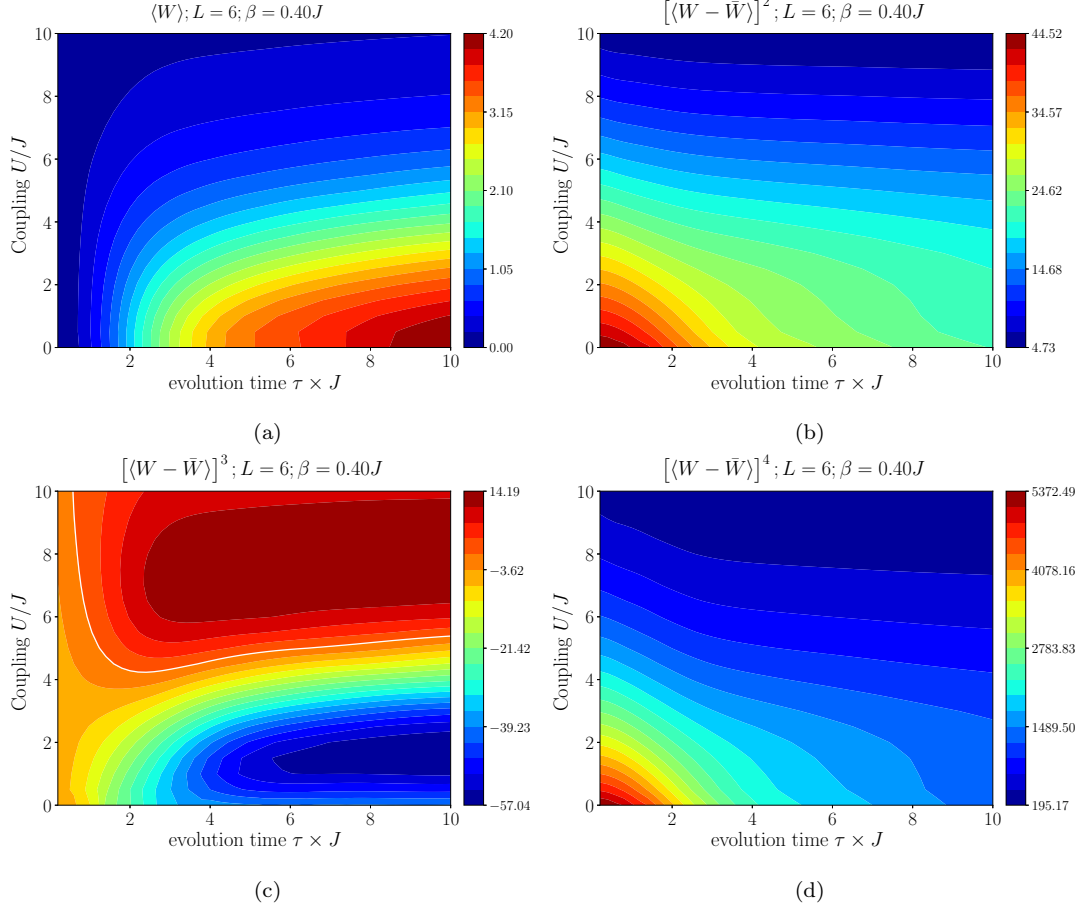


Figure 3: Heatmaps of the average work and the following three central momenta $\langle W - \bar{W} \rangle^k$ $k = 2, 3, 4$ for $L = 6$.

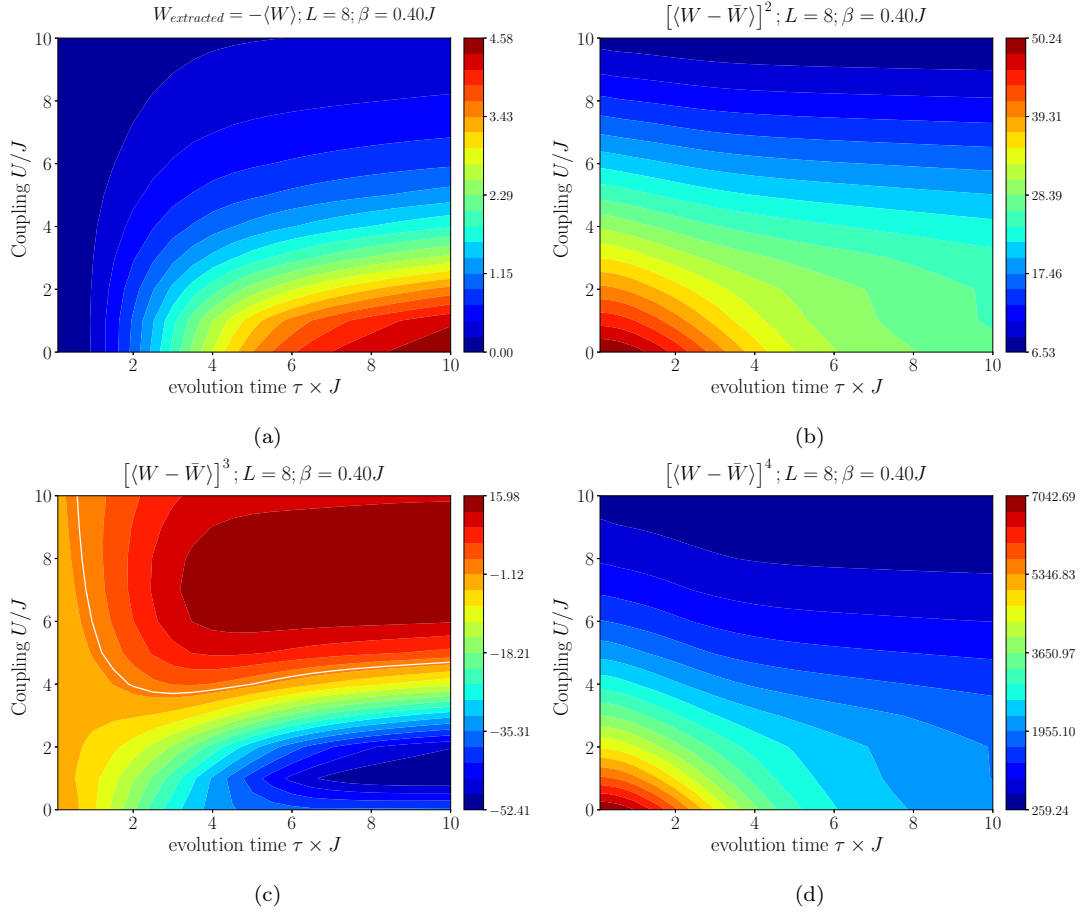


Figure 4: Heatmaps of the average work and the following three central momenta $\langle W - \bar{W} \rangle^k$ $k = 2, 3, 4$ for $L = 8$.

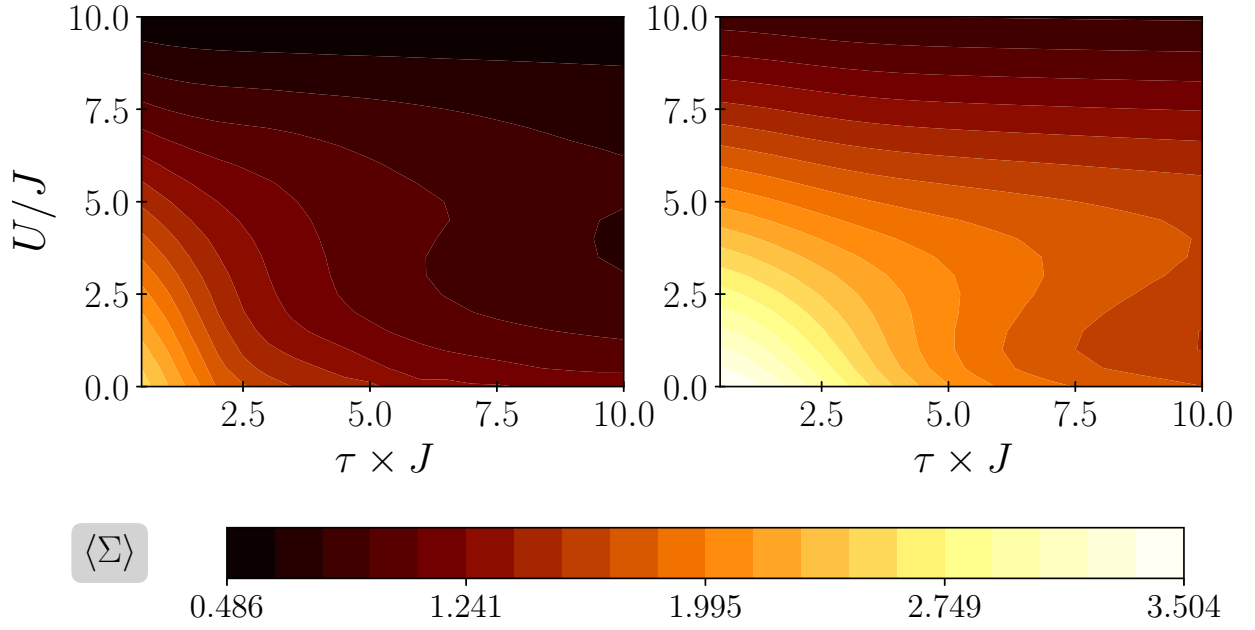


Figure 5: Heatmaps of the entropy production, for $L = 4$ (left) and $L = 8$ (right).

$L = 4, 6, 8$ is shown in Fig. 6. We note that in the not-scaled version the behavior of the curves are similar, depicting a minima followed by a maxima and a fast decay. Nonetheless, as stressed in the main text, the scaling behavior of the entropy with system size is not linear, and it is very sensitive to coupling regimes close to the quasi-QPT.

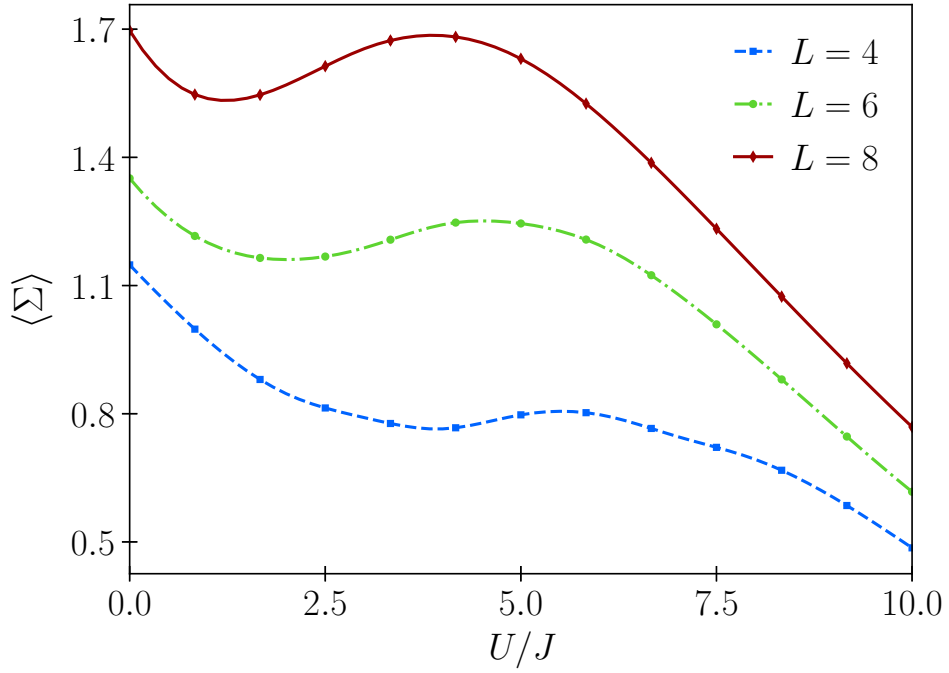


Figure 6: Entropy production as a function of the coupling U/J for $L = 4, 6, 8$.